Angewandte Chemie
Eine Zeitschrift der Gesellschaft Deutscher Chemiker

Supporting Information

69451 Weinheim, Germany

Starving the Malaria Parasite: A New Class of Inhibitors Active Against the Aspartic Proteases Plasmepsins I, II, and IV

Fraser Hof, Andri Schütz, Christoph Fäh, Solange Meyer, Daniel Bur, Jun Liu, Daniel E. Goldberg, and François Diederich*

1) Synthesis of inhibitor (±)-**1**, and precursors (±)-**2** and (±)-**3**.

All new compounds were characterized by m.p., IR, ^{1}H and ^{13}C NMR, and HRMS or elemental analysis.

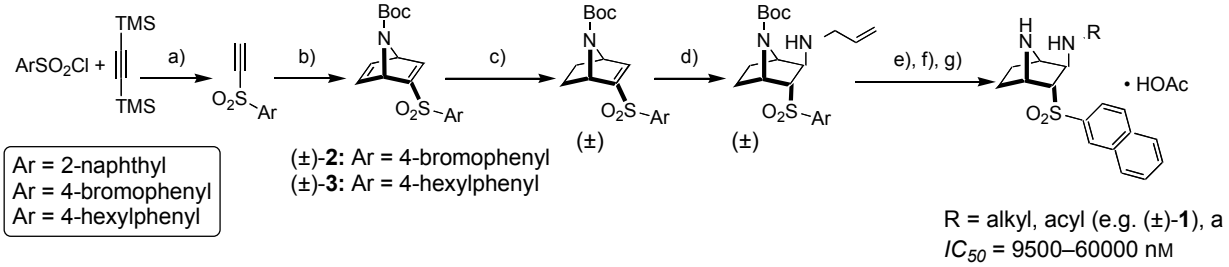

Scheme S1. Synthesis of the first generation of "diamine clamp" inhibitors by diastereoselective Michael-type addition of a primary amine to vinyl sulfones. a) $AlCl_3$, CH_2Cl_2, 0 → 22 °C, 16 h: then SiO_2; 30–76%. b) *N*-Boc pyrrole, 80 °C, 16 h; 51–76%. c) $Ni(OAc)_2$•$4H_2O$, $NaBH_4$, EtOH, THF, 22 °C, 16 h; 100%. d) Allylamine, Δ, 1 h; 86%. e) [$Pd(PPh_3)_4$], *N*,*N*'-dimethylbarbituric acid, CH_2Cl_2, 35 °C, 2.5 h; 65%. f) Reductive alkylation, acylation, or Cu-catalyzed arylation. g) TBSOTf, 2,6-lutidine, CH_2Cl_2, 22 °C, 30 min: then HOAc, CsF, DMF, 22 °C, 30 min; 88–99%. TBSOTf = *t*-butyldimethylsilyl trifluoromethanesulfonate, Boc = *t*-butoxycarbonyl.

2) Conformational analysis of phenyl sulfones.[1]

A Cambridge Structural Database search (CSD version 5.26, November 2004, limited to results that are not disordered, contain no ions, and contain no organometallics) for molecules containing the aryl sulfone fragment pictured below (Figure S1) provided 896 hit structures with a total of 1229 occurrences of the aryl sulfone structural fragment. 1125 of the fragments fall within $40° \leq |\theta_{C1\text{-}S\text{-}C2\text{-}C3}| \leq 140°$, with a clear maximum at 90°. Furthermore, 100 of the 104 occurrences of $|\theta_{C1\text{-}S\text{-}C2\text{-}C3}|$ outside of the range $40° \leq |\theta_{C1\text{-}S\text{-}C2\text{-}C3}| \leq 140°$ arise due to the constraints imposed within multicyclic aryl sulfones.

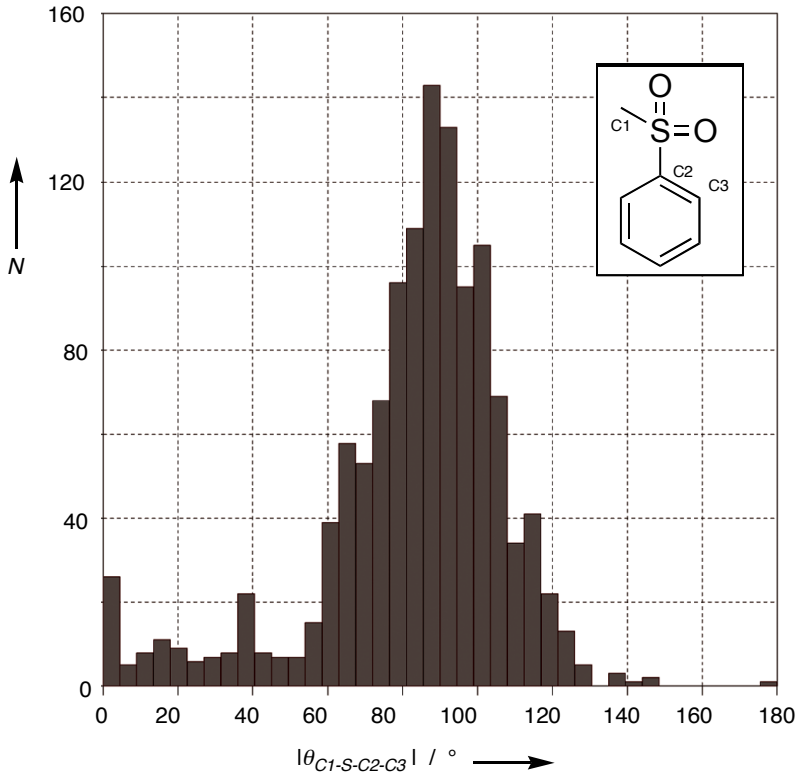

Figure S1. A histogram of dihedral angle occurrences in the CSD for the pictured aryl sulfone fragment.

3) Biochemical/biological evaluation of inhibition.

3a) Assays of in vitro enzyme activity – Washington University.
Analysis was carried out as previously reported.[2] Briefly, purified enzyme (Plasmepsin I or II, 1 nM) was incubated with a fluorescently labeled peptide substrate (1 mM) and varying concentrations of inhibitor (0–2800 nM) in pH 5.1 acetate buffer (100 mM). The amount of peptide cleavage, as determined by fluorescence measurements, at each concentration of inhibitor was fit to the Hill equation[2] to give the IC_{50} value for each inhibitor/enzyme combination. Data reported in the Table are the average of triplicate runs.

3b) Assays of in vitro enzyme activity – Actelion Pharmaceuticals.
Analysis was carried out as above using Plasmepsins II and IV, and human Cathepsins D and E, except that the experiments were carried out in pH 5.0 acetate buffer (50 mM) containing glycerol (12.5%), Me_2SO (10%), and BSA (0.1%). Data reported in the Table are the average of duplicate or triplicate runs.

3c) Assay of activity against cultured parasites – Washington University.
The assay was carried out as previously described.[3] Briefly, a culture of *Plasmodium falciparum* (clone 3D7) in red blood cells was incubated with inhibitor, followed by treatment with ^{3}H-hypoxanthine (a nucleic acid precursor required for parasite growth). Cells were isolated by filtration, and the amount of radioactive hypoxanthine taken up by the cells was determined by scintillation counting of the dry filters. The growth curves are shown in Figure S2.

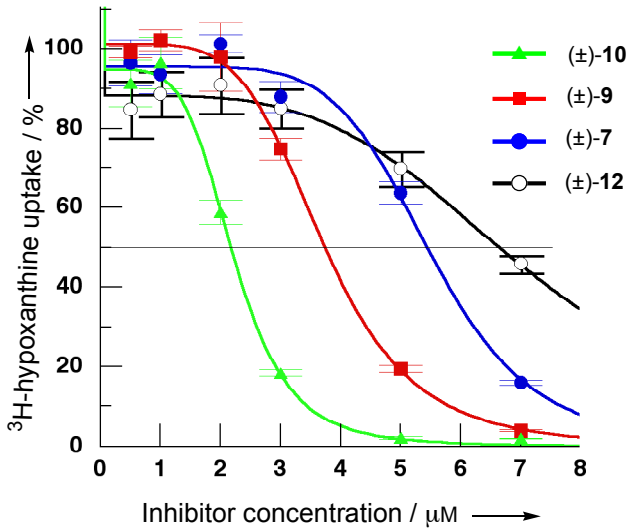

Figure S2. Dose-dependent growth of cultured *Plasmodium falciparum* as indicated by ^{3}H-hypoxanthine uptake. Data points are the average of three determinations at each concentration.

4) Modeling of inhibitors using MOLOC.

Potential inhibitors were manually docked within the known *flap*-open structures of PM II,[4,5] the enzyme structure was fixed, and the energy of the system was minimized using the MAB force field as implemented in the program MOLOC.[6] Comparative evaluation of inhibitors was based on 1) avoidance of unfavorable steric contacts, 2) maximum formation of favorable hydrogen bonding contacts, 3) complete filling of space within the binding pockets, and 4) the avoidance of energetically unfavorable conformations (e.g. gauche alkanes, and the aforementioned aryl sulfone constraint) for the inhibitor.

Minimized structures for both enantiomers of **12** in the active site of PM II are shown in Figure S3. Both structures can provide geometrically reasonable filling of space within the *flap* pocket, with the 2*S*,3*R* enantiomer (yellow) conforming more closely to the contours of the pocket in the region of Ile123 and Trp41. The bromobenzyl substituent of the 2*S*,3*R* enantiomer (yellow) forms favorable contacts within the hydrophobic *S1*/*S3* pocket, including key residues Phe111 and Phe120. The 2*R*,3*S* enantiomer (cyan), on the other hand, positions its bromobenzyl binding element in the extremely hydrophilic region pictured at left. Little favorable binding energy is expected to arise from the positioning of the hydrophobic bromobenzyl substituent within such an environment.

Additional evidence suggesting that the 2*S*,3*R* enantiomer (yellow) is the active component is provided if one assumes that all of the related inhibitors reported herein bind in a similar mode. The inhibitors in which the bromobenzyl group is replaced with 2-naphthylmethyl ((±)-**7**) or biphenylmethyl ((±)-**9** and (±)-**10**) substituents are also potent inhibitors of PM II. These substituents can easily be accommodated within the spacious *S1*/*S3* pocket, while the more compact hydrophilic pocket at left is too small to host these larger residues (models not shown).

Taken together with the > 70-fold greater activity against PM II for (–)-**12** relative to (+)-**12**, these results suggest that (–)-**12** be assigned as the 2*S*,3*R* enantiomer (yellow). The definitive assignment of enantiomers awaits further crystallographic or spectroscopic studies.

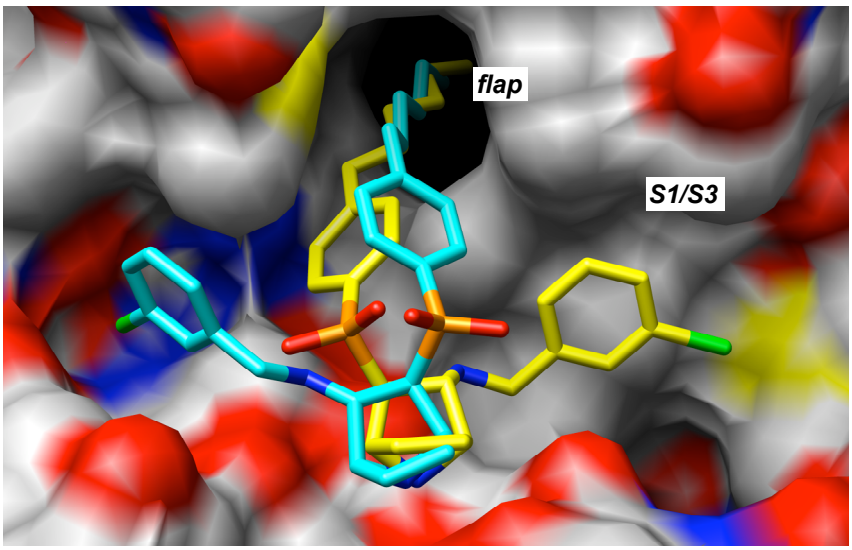

Figure S3. MOLOC-optimized structures of the two enantiomers of **12** within the active site of PM II (PDB code 2BJU). The 2*S*,3*R* enantiomer is depicted with yellow carbon atoms, while the 2*R*,3*S* enantiomer is pictured with cyan carbon atoms. The solvent-accessible surface of PM II is colored according to atom. Carbon = gray (or yellow/cyan for the two inhibitors), oxygen = red, nitrogen = blue, sulfur = orange, bromine = green. Hydrogen atoms and some protein residues that obscure the view of the *flap* pocket have been omitted for clarity. The surface was created using MSMS,[7] and the image was produced using Chimera.[8]

References

[1] This analysis closely follows a suggestion of Dr. Klaus Müller, F. Hoffman-La Roche, Basel.
[2] K. E. Luker, S. E. Francis, I. Y. Gluzman, D. E. Goldberg, *Mol. Biochem. Parasit.* **1996**, *79*, 71–78.
[3] I. Y. Gluzman, S. E. Francis, A. Oksman, C. E. Smith, K. L. Duffin, D. E. Goldberg, *J. Clin. Invest.* **1994**, *93*, 1602–1608.
[4] L. Prade, A. F. Jones, C. Boss, S. Richard-Bildstein, S. Meyer, C. Binkert, D. Bur, *J. Biol. Chem.* **2005**, *280*, 23837–23843.
[5] J. Yuvaniyama, A. D'Arcy, C. Öfner, H. Lötscher, D. Bur, G. E. Dale, H. P. Märki, F. K. Winkler, R. P. Moon, R. G. Ridley, in *Symposium on "Parasite proteases as drug targets"*, University of Glasgow, UK, **2000**.
[6] P. R. Gerber, K. Müller, *J. Comput.-Aided Mater. Des.* **1995**, *9*, 251-268.
[7] M.F. Sanner, A.J. Olson, J.C. Spehner, *Biopolymers* **1996**, *38*, 305–320.
[8] Molecular graphics images were produced using the Chimera package from the Computer Graphics Laboratory, University of California, San Francisco (supported by NIH P41 RR-01081): a) C.C. Huang, G.S. Couch, E.F. Pettersen, T.E. Ferrin, *Pacific Symposium on Biocomputing* **1996**, *1*, 724; b) http://www.cgl.ucsf.edu/chimera.